Proceedings of 14th IOE Graduate Conference
Peer Reviewed
Year: 2023 Month: December Volume: 14
ISSN: 2350-8914 (Online), 2350-8906 (Print)

Free Vibration Analysis of Multidisc Cantilever Shaft System

Kabita Ojha [a], Mahesh Chandra Luintel [b]

[a] *Department of Automobile and Mechanical Engineering, Thapathali Campus, IOE, Tribhuvan University*
[b] *Department of Mechanical and Aerospace Engineering, Pulchowk Campus, IOE, Tribhuvan University*
[a] kabitaojha55@gmail.com, [b] mcluintel@ioe.edu.np

Abstract
Cantilever shaft system is beneficial in various mechanical engineering application to transmit torque and rotational motion from power source to various components. The cantilever shaft with multiple disc is particularly used for limited space application and specific requirements configuration.The overall performance and safety of the system is reduced due to the excessive vibration and resonance. Mathematical model of the multidisc cantilever system is developed using Extended Hamilton's Principle and validate it through the ANSYS simulation. Different mode shapes and vibration behavior are observed during analysis and compare the result with mathematical solution. The critical speed obtained from the analytical method is close to simulation result.

Keywords
Multidisc, Extended Hamilton's Principle, Critical Speed, Forward Whirl, Backward Whirl

1. Introduction

Most of the mechanical engineering applications use a cantilever system, such as turbine, drive system, centrifugal pump etc. For the transmission of rotational motion and torque from a power source to various components the cantilever shaft system is used. Cantilever shaft with multidisc system is advantageous to enhance the efficiency and capacity of the overall system. The free vibration analysis of cantilever shaft system helps to avoid excessive vibrations, structural failures and resonance. The outcomes of this research will contribute to the optimization of multidisc cantilever shaft systems, ensuring their structural integrity, performance, and reliability in real-world applications.

The response of multidisc cantilever shaft system depends on the material properties, geometry of the discs, disc spacing, applied force, rotational velocity etc. These factors affect the natural frequency of the system, response amplitude, mode shapes and critical speeds. Several research have been conducted for the analysis of free vibration of shaft under varying load conditions and end conditions. An analysis of dynamics response of continuous shaft with different end conditions [1]. In this paper, the equation of motion for simply supported shaft and both end fixed shaft were developed using the Hamilton's principle. The critical frequency for both the cases are analyzed and found that the rate of increase of critical speed is more for simply supported shaft as compared with the both end fixed shaft.Polynomial mode shape functions were developed for continuous shafts with various end conditions[2]. There are various methods such as Galerkin method, assumed mode method, finite element method, Rayleigh-Ritz method etc. used to determine the vibration response of continuous system. In this paper, polynomial shape functions for continuous shaft with different end conditions were developed and compared with the result obtained from classical algebraic method. Lee et al. [3] used assumed modes method to analyzed the vibration of a rotor with multiple flexible disks. The shafts of steam turbine or computer storage devices mainly consist of multiple disks. The disk's flexibility and centrifugal stiffening were considered when designing the model. A modal analysis was conducted on a computer's hard disk drive spindle system and simple flexible rotors consisting of two disks. From this analysis, it was clear that the dynamic coupling between the shaft and the disk is significantly influenced by the fundamental mode of the system. Afshari et al. [4] analyzed an exact closed form solution for analyzing whirl behavior in Timoshenko rotors featuring multiple concentrated masses. For mathematical modeling of Timoshenko rotors with number of concentrated masses, Dirac's delta function was used. The frequency equation was derived by considering the various boundary conditions and corresponding mode shapes were calculated. From the analysis, it was found that the value of forward frequencies increases and backward frequencies decreases with the increase of rotational speed by considering the gyroscopic effect. Pokharel et al. [5] carried out an investigation into the free vibration dynamic response of overhung pelton turbine unit. The primary focus of the research is on modelling of pelton turbine unit with a rigid runner mounted on a circular flexible shaft supported by bearings. The objective is to assess the system's natural frequency using various modeling approaches. In the discrete system model, a simplified Jeffcott rotor model and Rayleigh's energy method were applied, while the continuous model involved the calculation of kinetic and potential energy for the runner, bucket and shaft. The Langrange's equations were used to formulate the governing equation and Rayleigh-Ritz method was used to solve the equation. Finally, the final results of critical frequencies for backward whirl and forward whirl were compared by simulating the model in ANSYS software.

Nirmall et al. [6] conducted an analysis of the free vibration characteristics of cantilever beams constructed from a variety of materials. All types of materials have some amount of internal damping. In this research, different materials such as aluminum, mild steel and brass were used for the free

vibration analysis. The natural frequencies of cantilever beams made from all the materials were calculated mathematically and experimentally. Then, the result were compared with the harmonic analysis performed in ANSYS software. The vibration analysis of tapered beam was conducted by Rishi Kumar Shukla [7]. The natural frequency of the double tapered cantilever Euler beam is derived using equation of motion. Weighted residual and Galerkin's method are used for finite element formulation of the beam and to determine the natural frequency and mode shapes. Cantilever beams with different taper ratios are used for the calculation and the frequencies and mode shapes are compared for different cases. Hosseini et al. [8]investigated the solution in multiple scales for analyzing the free vibrations of a rotating shaft exhibiting stretching non-linearity. In this paper, gyroscopic effect and rotary effect are considered while shear deformation is neglected. The equation of motion is derived using Hamilton's principle.The method of multiple scales method is used to solve the partial differential equation and determining the free vibration of the shaft. Both forward and backward nonlinear natural frequencies are calculated and then compared with the numerical simulations.

Previous studies have focused on the dynamic response analysis of cantilever beams and shafts without considering the multidisc configuration. However, limited research has been conducted specifically on the dynamic behavior of multidisc shaft systems. Therefore, there is a clear need to comprehensively investigate and understand the vibration analysis of multidisc cantilever shaft system.

2. Methodology

2.1 Mathematical Model

Assuming that the disc is rigid and considering only the kinetic energy of the disc. Initially, an inertial coordinate system denoted as X,Y and Z is defined, along with coordinate system represented by , x, y and z, which are fixed at the centre of the disc as shown in figure 1.

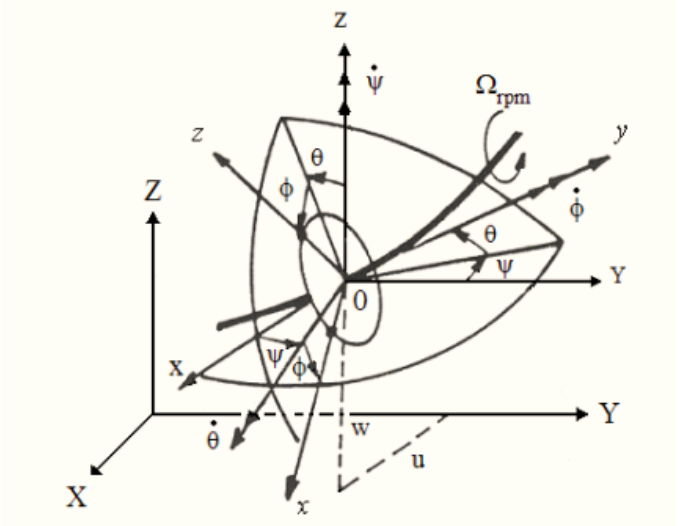

Figure 1: Coordinate System for a flexible shaft with a Rotating Disc

The mathematical modelling is started by considering the angular speed vector [wx, wy, wz] about the reference frame xyz fixed to the disc. [9]

$$\begin{bmatrix} w_x \\ w_y \\ w_z \end{bmatrix} = \begin{bmatrix} -\dot{\psi}\cos\theta\sin\phi + \dot{\theta}\cos\phi \\ \dot{\phi} + \dot{\psi}\sin\theta \\ \dot{\psi}\cos\theta\cos\phi + \dot{\theta}\sin\phi \end{bmatrix} \quad (1)$$

Where, θ, Ψ, ϕ = Euler angles
The displacements of the disk's center of mass along the directions X and Z of the inertial reference frame respectively by u and w. θ and Ψ are very small
Ω = rate of spin

$$\begin{bmatrix} w_x \\ w_y \\ w_z \end{bmatrix} = \begin{bmatrix} -\dot{\psi}\cos\theta\sin\phi + \dot{\theta}\cos\phi \\ \dot{\phi} + \dot{\psi}\sin\theta \\ \dot{\psi}\cos\theta\cos\phi + \dot{\theta}\sin\phi \end{bmatrix} = \begin{bmatrix} -\dot{\psi}\phi + \dot{\theta} \\ \Omega + \dot{\psi}\theta \\ \dot{\psi} + \dot{\theta}\phi \end{bmatrix} \quad (2)$$

The equation (3) represents the disc's kinetic energy.

$$\boldsymbol{T_D} = 1/2\boldsymbol{M_D}\left(\dot{\boldsymbol{u}}^2 + \dot{\boldsymbol{w}}^2\right) + 1/2\left(\boldsymbol{I_{Dx}}\boldsymbol{w_x^2} + \boldsymbol{I_{Dy}}\boldsymbol{w_y^2} + \boldsymbol{I_{Dz}}\boldsymbol{w_z^2}\right) \quad (3)$$

Where, M_D = Mass of the disk
I_Dx, I_Dy, I_Dz = Inertia of disk of about principle axis xyz
$I_Dx = I_Dz$
After simplification, the equation (3) becomes,

$$\boldsymbol{T_D} = 1/2\boldsymbol{M_D}\left(\dot{\boldsymbol{u}}^2 + \dot{\boldsymbol{w}}^2\right) + 1/2\boldsymbol{I_{Dx}}\left(\dot{\boldsymbol{\theta}}^2 + \dot{\boldsymbol{\psi}}^2\right) + 1/2\boldsymbol{I_{Dy}}\left(\boldsymbol{\Omega}^2 + 2\boldsymbol{\Omega}\dot{\boldsymbol{\psi}}\boldsymbol{\theta}\right) \quad (4)$$

There are total three disc in consideration. Here, kinetic energy of each disc is calculated. Equation (5) provides the expression for the kinetic energy of the first disk.

$$T_{d1} = 1/2M_{D1}\int_0^L \left(\dot{u}^2 + \dot{w}^2\right)\delta_d\left(y - \frac{L}{3}\right)\mathrm{dy} + 1/2I_{D1x}\int_0^L \left(\dot{\theta}^2 + \dot{\psi}^2\right) \delta_d\left(y - \frac{L}{3}\right)\mathrm{dy} + 1/2I_{D1y}\int_0^L \left(\Omega^2 + 2\Omega\dot{\psi}\theta\right)\delta_d\left(y - \frac{L}{3}\right)\mathrm{dy} \quad (5)$$

Equation (6) represents the kinetic energy of the second disc.

$$T_{d2} = 1/2M_{D2}\int_0^L \left(\dot{u}^2 + \dot{w}^2\right)\delta_d\left(y - \frac{2L}{3}\right)dy + 1/2I_{D2x}\int_0^L \left(\dot{\theta}^2 + \dot{\psi}^2\right) \delta_d\left(y - \frac{2L}{3}\right)dy + 1/2I_{D2y}\int_0^L \left(\Omega^2 + 2\Omega\dot{\psi}\theta\right)\delta_d\left(y - \frac{2L}{3}\right)dy \quad (6)$$

Equation (7) describes the kinetic energy of the third disc.

$$T_{d3} = 1/2M_{D3}\int_0^L \left(\dot{u}^2 + \dot{w}^2\right)\delta_d(y - L)\mathrm{dy} + 1/2I_{D3x}\int_0^L \left(\dot{\theta}^2 + \dot{\psi}^2\right) \delta_d(y - L)\mathrm{dy} + 1/2I_{D3y}\int_0^L \left(\Omega^2 + 2\Omega\dot{\psi}\theta\right)\delta_d(y - L)\mathrm{dy} \quad (7)$$

The shaft is influenced by both the kinetic and potential energy. The expression in equation (4) is kinetic energy of the shaft and equation (5) is related to potential energy of the shaft, where L is the length of the shaft. Equation (8) provides the expression for the kinetic energy of the shaft.

$$T_s = 1/2\rho_s A_s\int_0^L \left(\dot{u}^2 t\dot{w}^2\right)\mathrm{dy} + 1/2\rho_s I_s\int_0^L \left(\dot{\theta}^2 + \dot{\psi}^2\right)\mathrm{dy} + \rho I_s L\Omega^2 + 2\rho I_s\Omega\int_0^L \dot{\psi}\theta\mathrm{dy} \quad (8)$$

Equation (9) expresses the potential energy of the shaft.

$$\mathrm{V} = 1/2\mathrm{E}\boldsymbol{I}_{zz}\int_0^L \left[\left(\boldsymbol{u}''\right)^2 + \left(\boldsymbol{w}''\right)^2\right]\mathrm{dy} \tag{9}$$

The cumulative kinetic energy of the system is determined by summing up equation (5), equation (6), equation (7) and equation (8).

$$\begin{aligned}
&\mathrm{T} = 1/2M_{D1}\int_0^L \left(\dot{u}^2 + \dot{w}^2\right)\delta_d\left(y-\frac{L}{3}\right)\mathrm{dy} + 1/2I_{D1x}\\
&\int_0^L \left(\dot{\theta}^2 + \dot{\psi}^2\right)\delta_d\left(y-\frac{L}{3}\right)\mathrm{dy} + 1/2I_{D1y}\int_0^L \left(\Omega^2 + 2\Omega\dot{\psi}\theta\right)\delta_d\\
&\left(y-\frac{L}{3}\right)\mathrm{dy} + 1/2M_{D2}\int_0^L \left(\dot{u}^2 + \dot{w}^2\right)\delta_d\left(y-\frac{2L}{3}\right)\mathrm{dy} + 1/2I_{D2x}\\
&\int_0^L \left(\dot{\theta}^2 +)\ \dot{\psi}^2\right)\delta_d\left(y-\frac{2L}{3}\right)\mathrm{dy} + 1/2I_{D2y}\int_0^L \left(\Omega^2 + 2\Omega\dot{\psi}\theta\right)\delta_d\\
&\left(y-\frac{2L}{3}\right)\mathrm{dy} + 1/2M_{D3}\int_0^L \left(\dot{u}^2 + \dot{w}^2\right)\delta_d(y-L)\mathrm{dy} + 1/2I_{D3x}\\
&\int_0^L \left(\dot{\theta}^2 + \dot{\psi}^2\right)\delta_d(y-L)\mathrm{dy} + 1/2I_{D3y}\int_0^L \left(\Omega^2 + 2\Omega\dot{\psi}\theta\right)\delta_d\\
&(y-L)\mathrm{dy} + 1/2\rho_s A_s\int_0^L \left(\dot{u}^2 + \dot{w}^2\right)\mathrm{dy} + 1/2\rho_s I_s\int_0^L \left(\dot{\theta}^2 + \dot{\psi}^2\right)\mathrm{dy}\\
&+ \rho I_s\mathbf{L}^2 + 2\rho I_s\Omega\int_0^L \dot{\psi}\theta\, dy
\end{aligned} \tag{10}$$

Now, applying Extended Hamilton's Principle:

$$\delta\int_{t1}^{t2}(L + W_{nc})\, dt = 0 \tag{11}$$

The equation of motion is

$$\begin{aligned}
&M_{D1}\ddot{u}\delta_d\left(y-\frac{L}{3}\right) + M_{D2}\ddot{u}\delta_d\left(y-\frac{2L}{3}\right) + M_{D3}\ddot{u}\delta_d(y-L) -\\
&I_{D1y}\ddot{u}''\delta_d\left(y-\frac{L}{3}\right) - I_{D2y}\ddot{u}''\delta_d\left(y-\frac{2L}{3}\right) - I_{D3y}\ddot{u}''\delta_d(y-L) +\\
&I_{D1y}\Omega\dot{w}''\delta_d\left(y-\frac{L}{3}\right) + I_{D2y}\Omega\dot{w}''\delta_d\left(y-\frac{2L}{3}\right) + I_{D3y}\Omega\dot{w}''\\
&\delta_d(y-L) + \rho_s A_s\ddot{u} - \rho_s I_s\ddot{u}'' + 2\rho I\Omega\dot{w}'' + EI_{zz}u^{iv} = 0
\end{aligned} \tag{12}$$

$$\begin{aligned}
&M_{D1}\ddot{w}\delta_d\left(y-\frac{L}{3}\right) + M_{D2}\ddot{w}\delta_d\left(y-\frac{2L}{3}\right) + M_{D3}\ddot{w}\delta_d(y-L) -\\
&I_{D1y}\ddot{w}''\delta_d\left(y-\frac{L}{3}\right) - I_{D2y}\ddot{w}''\delta_d(y-\frac{2L}{3}) - I_{D3y}\ddot{w}''\delta_d(y-L) +\\
&I_{D1y}\Omega\dot{u}''\delta_d\left(y-\frac{L}{3}\right) + I_{D2y}\Omega\dot{u}''\delta_d\left(y-\frac{2L}{3}\right) + I_{D3y}\Omega\dot{u}''\delta_d(y-L)\\
&+ \rho_s A_s\ddot{w} - \rho_s I_s\ddot{w}'' + 2\rho I\Omega\dot{u}'' + EI_{zz}w^{iv} = F_1\delta_d\left(y-\frac{L}{3}\right) +\\
&F_2\delta_d\left(y-\frac{2L}{3}\right) + F_3\delta_d(y-L)
\end{aligned} \tag{13}$$

For further calculation, the parameters of the system shown in table 1 are used [10]. The main parameter are density of the shaft material,length of the shaft, cross-section area of the shaft, modulus of elasticity etc.

Table 1: Parameters of the System

S.N.	Parameters	Value
1	Density of shaft material	7680 kg/m^3
2	Cross-sectional area of the shaft	3.14 x 10^{-4} m^2
3	Length of the shaft	0.5 m
4	Modulus of Elasticity of shaft material	207 x 10^9 N/m^2
5	Area moment of inertia of the shaft section	7.85 x 10^{-9}
6	Moment of the shaft	0.0136 kg m^2
7	Mass of a disc	1.401 kg

The mode shape functions for a cantilever shaft shown in equation (14) is used to calculated modal mass,modal damping and modal stiffness.

$$\{\phi(x)\} = \begin{Bmatrix}\phi_1(x)\\ \phi_2(x)\end{Bmatrix} = \begin{Bmatrix} y^4 - 4Ly^3 + 6L^2y^2 \\ y^5 - \frac{661}{182}Ly^4 + \frac{412}{91}L^2y^3 - \frac{163}{91}L^3y^2\end{Bmatrix} \tag{14}$$

From equation (12) and (13), the model mass, model damping, and modal stiffness are obtained as shown in equations (15), (16) and (17).

$$\begin{aligned}
M_i = {} & M_{D1}\cdot\left(\phi_i(\mathrm{y})\right)^2\Big|_{y=\frac{L}{3}} + M_{D2}\cdot\left(\phi_i(\mathrm{y})\right)^2\Big|_{y=\frac{2L}{3}} +\\
& M_{D3}\cdot\left(\phi_i(\mathrm{y})\right)^2\Big|_{y=L} + \int_0^L \rho_s A_s\left(\phi_i(y)\right)^2 dy -\\
& \int_0^L \rho_s I_s\left(\phi_i''(y)\phi_1(y)\right) dy - I_{D1y}\left(\phi_i''(y)\phi_1(y)\right)\Big|_{y=\frac{L}{3}}\\
& - I_{D2y}\left(\phi_i''(y)\phi_1(y)\right)\Big|_{y=\frac{2L}{3}} - I_{D3y}\left(\phi_i''(y)\phi_1(y)\right)\Big|_{y=L}
\end{aligned} \tag{15}$$

$$\begin{aligned}
C_i = {} & I_{D1y}\Omega\left(\phi_i''(y)\phi_1(y)\right)\Big|_{y=L/3} + I_{D2y}\Omega\left(\phi_i''(y)\phi_1(y)\right)\Big|_{y=2L/3} +\\
& I_{D3y}\Omega\left(\phi_i''(y)\phi_1(y)\right)\Big|_{y=L} + 2\rho I_s\Omega\int_0^L \left(\phi_i''(y)\phi_1(y)\right) dy
\end{aligned} \tag{16}$$

$$K_i = \mathrm{E}I_s\int_0^L \phi_i^{iv}(y)\phi_i(y)\, dy \tag{17}$$

The calculations for the model mass, model damping, and modal stiffness for each mode of the cantilever shaft are performed using Maple software. Subsequently, additional calculations are conducted to determine the critical speeds for both forward and backward whirl for the first and second mode shape functions. The natural frequency corresponding to forward and backward whirl are calculated by using the formula [1] shown in equation (18) and (19). The critical speeds for both cases are listed in table 2 and table 3.

$$(\lambda_i)_1 = \sqrt{\frac{1}{2}\left[\left\{\left(\frac{C_i}{M_i}\right)^2 + 2\frac{K_i}{M_i}\right\} + \sqrt{\left(\frac{C_i}{M_i}\right)^4 + 4\left(\frac{C_i}{M_i}\right)^2\frac{K_i}{M_i}}\right]} \tag{18}$$

$$(\lambda_i)_2 = \sqrt{\frac{1}{2}\left[\left\{\left(\frac{C_i}{M_i}\right)^2 + 2\frac{K_i}{M_i}\right\} - \sqrt{\left(\frac{C_i}{M_i}\right)^4 + 4\left(\frac{C_i}{M_i}\right)^2\frac{K_i}{M_i}}\right]} \tag{19}$$

Table 2: Critical Speed for Forward Whirl

S.N.	Speed	First Mode (rad/s)	Second Mode (rad/s)	Ratio
1	0	139.69	756.68	5.42
2	500	142.28	811.99	5.7
3	1000	145.96	871.04	5.96
4	1500	149.74	933.74	6.23
5	2000	153.6	999.96	6.5
6	2500	157.56	1069.56	6.78
7	3000	161.6	1142.31	7.07
8	3500	165.73	1218.006	7.35
9	4000	169.94	1296.42	7.63

Table 3: Critical Speed for Backward Whirl

S.N.	Speed	First Mode (rad/s)	Second Mode (rad/s)	Ratio
1	0	139.69	756.68	5.42
2	500	135.19	705.15	5.21
3	1000	131.77	657.35	4.99
4	1500	128.45	613.2	4.77
5	2000	125,22	572,58	4,57
6	2500	122.08	535.33	4.38
7	3000	119.03	501.24	4.21
8	3500	116.06	470.09	4.05
9	4000	113.18	441.66	3.9

2.2 Simulation

Simulation was conducted to the validation of the mathematical model of the multidisc cantilever shaft system. For the simulation, a geometric model of the cantilever shaft system with discs was prepared using ANSYS software, as shown in Figure 2. Meshing of the model was performed as illustrated in Figure 3. A fixed support was added at the end of the cantilever shaft system, and rotational velocities ranging from 500 rpm to 3000 rpm were applied to the shaft for rotation. When the model was run to obtain a solution, it shows bending in the shaft for various mode shapes. The relationship between rotational velocity and frequency was observed through the Campbell diagram, as shown in Figure 4.

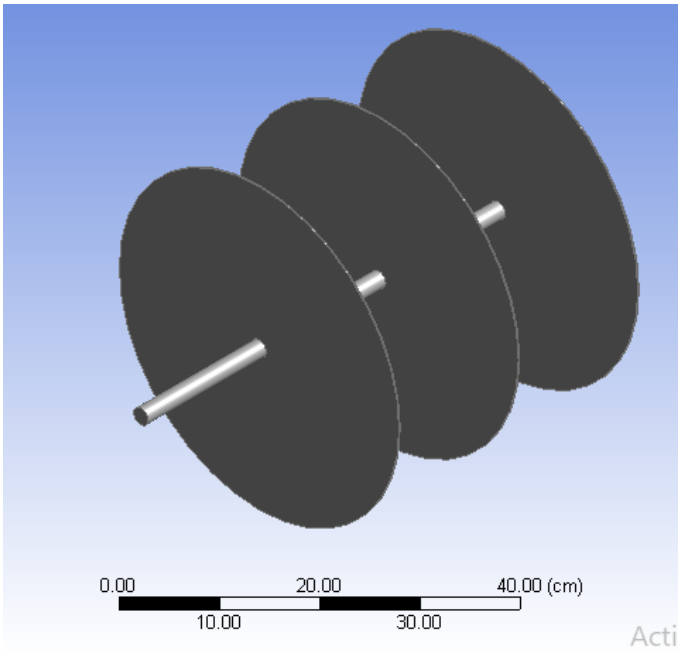

Figure 2: Geometric Model of the Cantilever Shaft with Discs

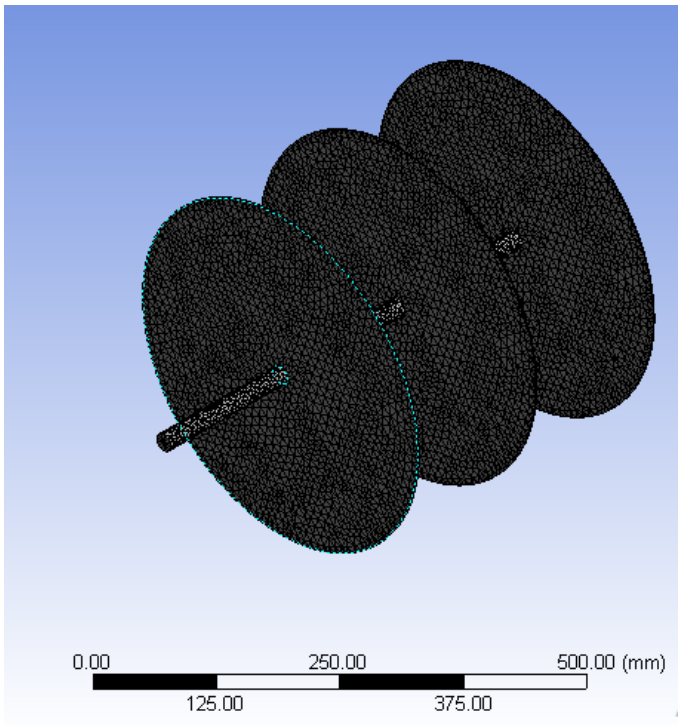

Figure 3: Meshing of the Geometric Model

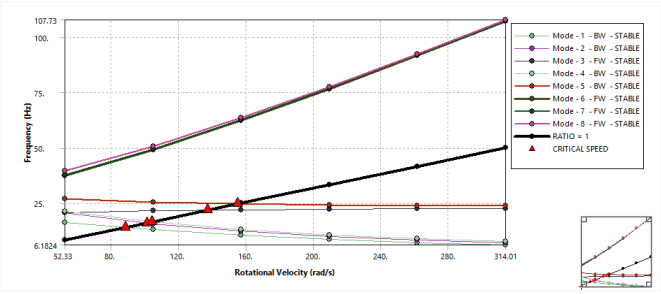

Figure 4: Campbell Diagram from ANSYS Simulation

3. Result and Discussion

3.0.1 Comparison between Analytical and Simulation Result

After completion of the mathematical calculation, the result obtained from the ANSYS simulation and mathematical calculation were compared with each other. The critical speed for forward whirl for first mode in both calculation and simulation is shown in table 4. Similarly, the critical speed for backward whirl for first mode in both calculation and analysis result is shown in table 5. From the both table it was found that the value of critical speed in both the cases are close to each other.

Table 4: Comparative Result of Damped Frequency for Forward Whirl

S.N.	Speed (rpm)	First Mode (Maple) Hz	First Mode (ANSYS) Hz
1	500	22.64	20.8
2	1000	23.23	21.58
3	1500	23.83	22.00
4	2000	24.45	22.26
5	2500	25.08	22.43
6	3000	25.72	22.56

Table 5: Comparative Result of Damped Frequency for Backward Whirl

S.N.	Speed (rpm)	First Mode(Maple) Hz	First Mode (ANSYS) Hz
1	500	21.52	26.37
2	1000	20.97	24.89
3	1500	20.44	24.25
4	2000	19.93	23.92
5	2500	19.45	23.71
6	3000	18.94	23.57

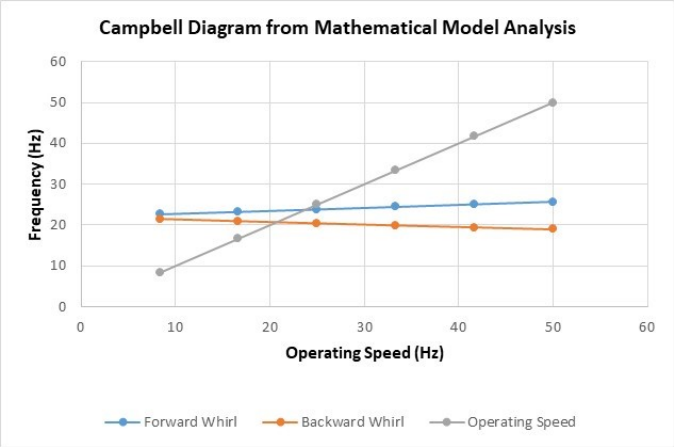

Figure 5: Campbell Diagram From Mathematical Model Analysis

From the above table it is clear that the critical speeds corresponding to forward whirl increases with the increase in operating speed in both mathematical calculation and simulation. On the other hand, the critical speeds corresponding to backward whirl decreases with the increase in operating speed in both the cases.

The relationship between frequency and operating speed obtained from mathematical model analysis is shown in Figure 5. The critical speed for forward and backward whirl is also calculated from the diagram. Similarly, the critical speed for both the forward and backward whirl shown in figure 6 is calculated in ANSYS software for the validation of the mathematical model. From the comparative study between both the mathematical and simulation result, it was found that the critical speed for both the cases were close to each other.

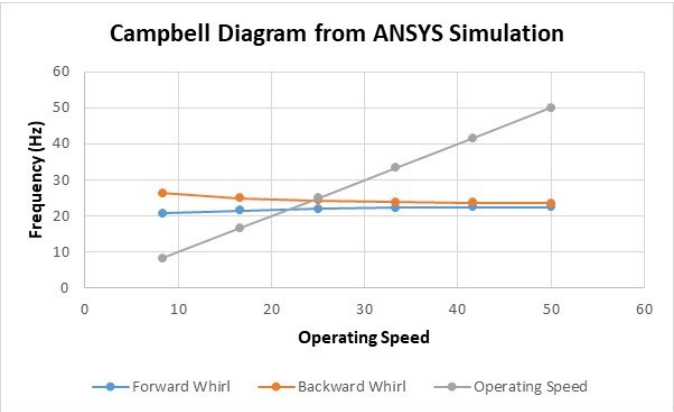

Figure 6: Campbell Diagram from ANSYS Simulation

4. Conclusion

The free vibration analysis of the multidisc cantilever shaft system was conducted by using two mode orthogonal shape functions. The mathematical model of the multidisc cantilever shaft system was prepared by using Extended Hamilton's principle. Both analytical and simulation method were employed to investigate the natural frequencies and mode shapes of the multidisc cantilever shaft system.

The value of critical speed for forward whirl in mathematical calculation was found to be 24 Hz. Similarly, the critical speed for backward whirl in mathematical calculation was found to be 21 Hz. Then, from simulation, the critical speed for forward whirl was found to be 22 Hz and critical speed for backward whirl was found to be 24 Hz.

After completion of the research, the critical speed obtained from both the mathematical calculation and simulation result were found to be close to each other.For the future work, boundary conditions and geometric properties of the shaft and disc will be modified and further analysis will be conducted.

Acknowledgments

This study would not have been accomplished without support and assistant-ship of college and professor team. The authors wish to express gratitude to all individuals who provided direct or indirect support throughout the research.

References

[1] Mahesh Chandra Luintel. Dynamic response of continuous shafts with different end conditions. *Journal of Innovations in Engineering Education| Vol*, 2(1), 2019.

[2] Mahesh Chandra Luintel. Development of polynomial mode shape functions for continuous shafts with different end conditions. *Journal of the Institute of Engineering*, 16(1):151–161, 2021.

[3] Chong-Won Lee and Sang-Bok Chun. Vibration analysis of a rotor with multiple flexible disks using assumed modes method. *Journal of Vibrationa and Acoustics*, 1998.

[4] Hassan Afshari, Keivan Torabi, and Adel Jafarzadeh Jazi. Exact closed form solution for whirling analysis of timoshenko rotors with multiple concentrated masses. *Mechanics Based Design of Structures and Machines*, 50(3):969–992, 2022.

[5] Kamal Pokharel and Mahesh Chandra Luintel. Dynamic response of overhung pelton turbine unit for free vibration. In *IOE Graduate Conference*, volume 6, pages 477–482, 2019.

[6] T Nirmall and S Vimala. Free vibration analysis of cantilever beam of different materials. *International Journal of Applied Engineering Research*, 5(4):612–615, 2016.

[7] Rishi Kumar Shukla. *Vibration analysis of tapered beam*. PhD thesis, 2013.

[8] SAA Hosseini and M Zamanian. Multiple scales solution for free vibrations of a rotating shaft with stretching nonlinearity. *Scientia Iranica*, 20(1):131–140, 2013.

[9] Carlos Alberto Bavastri, Euda Mara da S Ferreira, José João de Espíndola, and Eduardo Márcio de O Lopes. Modeling of dynamic rotors with flexible bearings due to the use of viscoelastic materials. *Journal of the Brazilian Society of Mechanical Sciences and Engineering*, 30:22–29, 2008.

[10] Hong-Cheng Sheu and Lien-Wen Chen. A lumped mass model for parametric instability analysis of cantilever shaft–disk systems. *Journal of sound and vibration*, 234(2):331–348, 2000.